ORGANIC CHEMISTRY FRONTIERS

RESEARCH ARTICLE

View Article Online
View Journal

Cite this: DOI: 10.1039/d5qo00508f

α-Sulfonylated ketazine synthesis from vinyl azides and sodium sulfinates using CAN: radical C–S/N–N coupling cascade as a key reaction pathway†

Mikhail M. Doronin, [a] Alexander S. Klikushin, [a,b] Olga M. Mulina, [a] Michael G. Medvedev, [a] Vera A. Vil', [a] Liang-Nian He [c] and Alexander O. Terent'ev *[a,b]

Received 15th March 2025,
Accepted 17th May 2025

DOI: 10.1039/d5qo00508f

rsc.li/frontiers-organic

Synthesis of α-sulfonylated ketazines from vinyl azides and sodium sulfinates proceeding *via* radical C–S/N–N coupling cascade has been developed. The cascade starts from the generation of sulfonyl radicals through RSO_2Na oxidation by cerium(IV) ammonium nitrate (CAN). Their addition to the double bond of vinyl azides, followed by N_2 elimination, leads to the formation of iminyl radicals, whose N–N coupling provides α-sulfonylated ketazines in yields up to 96%. This process represents one of the rare facets of iminyl radical reactivity, namely, N–N radical coupling while bypassing their reduction, intramolecular cyclization, and 1,*n*-HAT that are typical for them. The EPR-spectra study and quantum chemical calculations revealed that the selective N–N coupling of iminyl radicals was facilitated by the inertness of Ce(III) towards coordination with iminyl radicals and the inaccessibility of charge transfer. In contrast, Mn(II) coordinates with iminyl radicals and converts them into enamines.

1 Introduction

Radical coupling processes have become increasingly popular as an alternative to the nucleophile–electrophile strategy. Typically, radical species are generated by single-electron oxidants or reductants, which are often metal compounds prone to single-electron transfer. Therefore, unravelling the role of metal-based oxidants in radical processes is crucial, as the metal can significantly affect the formed radicals through coordination causing them to lose their radical character *via* charge transfer, *etc*.[1–6] Among all oxidants, Ce(IV)-based systems,[7] for example cerium(IV) ammonium nitrate (CAN),[8,9] have been broadly engaged in organic synthesis as single-electron oxidants. Nevertheless, the coordination of Ce(IV) and Ce(III) ions formed during reduction with radical species has been most often neglected. This research revealed a key difference between two commonly employed metal oxidants, CAN and $Mn(OAc)_3$, towards N-centered iminyl radicals.

Recently, iminyl radicals have been known to be generated from vinyl azides.[10–13] Due to the presence of a double bond and an azido group at the same carbon atom, vinyl azides can act not only as electrophiles/nucleophiles[14–18] but also as peculiar radical acceptors.[19–21] The addition of free carbon- and heteroatom-centred radicals to vinyl azides enables the formation of functionalized iminyl radicals by means of N_2 elimination (Scheme 1A).[10–12] Using these unique chemical properties of vinyl azides, a variety of compounds have already been synthesized, such as pyrroles,[22] pyridines,[23] isoquinolines,[24] β-functionalized ketones[19,25] and enamines,[26–28] *etc*. In most cases, the generated iminyl radicals can induce 1,*n*-HAT processes on remote C–H bonds[25,29] (Scheme 1A (1)) or undergo intramolecular radical cyclization *via* addition to the π-systems[30,31] (Scheme 1A (2)). In addition, iminyl radicals can easily be converted to imines because of reduction, intra- or intermolecular HAT processes, followed by tautomerization,[26,32] cyclization,[33] or hydrolysis[19] (Scheme 1A (3)). In particular, the coordination of generated iminyl radicals on metal ions with subsequent metal-to-ligand charge transfer (MLCT) was proposed as the main path for the metal oxidant turnover.[22,23,33,34] Given this, iminyl radicals have

[a]*Zelinsky Institute of Organic Chemistry, Russian Academy of Sciences, 47 Leninsky Prospect, Moscow, 119991, Russian Federation. E-mail: terentev@ioc.ac.ru; Tel: (+7)-499-137-2944*
[b]*Mendeleev University of Chemical Technology of Russia, 9 Miusskaya Square, Moscow 125047, Russian Federation*
[c]*State Key Laboratory and Institute of Elemento-Organic Chemistry, Frontiers Science Center for New Organic Matter, College of Chemistry, Nankai University, Tianjin 300071, China*

†Electronic supplementary information (ESI) available: General reaction procedures, characterization data, copies of NMR spectra. CCDC 2429110. For ESI and crystallographic data in CIF or other electronic format see DOI: https://doi.org/10.1039/d5qo00508f

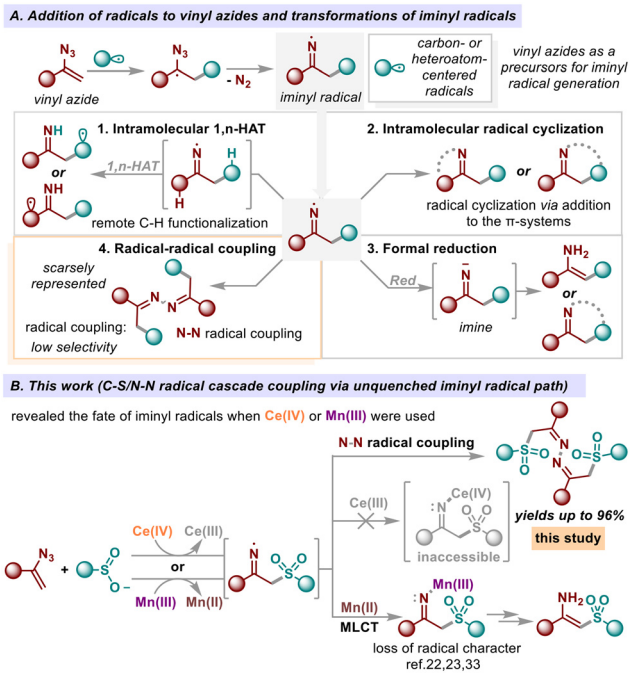

Scheme 1 Radical transformations of vinyl azides.

been engaged as universal intermediates for radical relay catalysis.[35] By way of contrast, the N–N radical coupling of iminyl radicals was scarcely represented due to their propensity to the reduction step, resulted in imine intermediates (Scheme 1A (4)). In addition, the direct coupling of two radicals is hard to achieve, due to low selectivity and side-processes of radical decay.

Approach based on radical sulfonylation has emerged as an effective alternative for the synthesis of organosulfur compounds.[36–38] Sulfones are widely represented in numerous commercially available drugs,[39] functional materials,[40,41] and agrochemicals.[42] Showcasing multifaceted bioisosterism,[43,44] these compounds have gained extensive interest owing to their variety of valuable properties, such as enhanced lipophilicity and metabolic stability.[45] In this regard, application of sulfonyl radicals may ensure peculiar radical selectivity[36,46] and high functional group tolerance, paving the way for the late-stage functionalization[47] and enhanced molecular complexity of targeting compounds.[48–50] Previously, it was shown that generated sulfonyl radicals could be effectively intercepted by vinyl azides resulting in the formation of β-ketosulfones[51] and *N*-unsubstituted enaminosulfones.[27,52,53] Later, Liu and co-workers reported transformation proceeding *via* formal 1,3-HAT/radical coupling cascade which provided *gem*-disulfonyl enamines.[28] Notably, in all the aforementioned studies, the N–N coupling process of iminyl radicals was not observed. By way of contrast, Chiba and co-workers have found that CF_3-radicals generated from Me_3SiCF_3 under oxidation by means of $PhI(OAc)_2$ could induce process of iminyl radicals N–N coupling leading to the diastereoisomeric mixture of α-trifluoromethylated ketazines.[24]

Herein, we have discovered radical C–S/N–N cascade coupling induced by addition of sulfonyl radicals to vinyl azides (Scheme 1B), resulting in the formation of potentially valuable α-sulfonylated ketazines,[54–56] being a rare example of iminyl radicals N–N coupling process. Noteworthy, the similar process mediated by $Mn(OAc)_3$ provided enaminosulfones (Scheme 1B).[27] For these reasons, the main goal of recent research to elucidate the key factors that govern the distinguishable reactivity of cerium and manganese salts towards generated iminyl radicals and led to different reaction products from the same starting substrates (Scheme 1B).

2 Results and discussion

2.1 Optimization and scope of substrates

We commenced our study with the search of optimal reaction conditions. For this purpose, (1-azidovinyl) benzene **1a** and sodium benzenesulfinate **2a** were chosen as model substrates (Table 1). The influence of CAN amount, reaction time, solvent nature, and starting reagents molar ratio on the sulfonylated product **3aa** yield was tested. The reaction between **1a** and **2a** for 60 minutes with the addition of 1 equivalent of CAN in DMSO-THF gave sulfonylated azine **3aa** in a 73% yield (entry 1). Its structure was unambiguously confirmed by X-ray ana-

Table 1 Optimization of the reaction conditions for the synthesis of sulfonyl azine **3aa** from vinyl azide **1a** and sodium sulfinate **2a**[a]

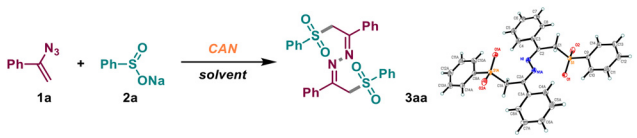

Entry	Molar ratio **1a** : **2a**, (mol : mol)	CAN (eq.)	Solvent	Time, min	**3aa** yield,[b] %
1	1 : 1	1	DMSO–THF	60	73
2	1 : 1	0.5	DMSO–THF	60	43
3	1 : 1	1.5	DMSO–THF	60	80
4	1 : 1	1.5	DMSO–THF	30	67
5	1 : 1	1.5	DMSO–THF	90	76
6[c]	1 : 1	1.5	DMSO–THF	60	71
7	1 : 1	1.5	DMSO–MeCN	60	61
8	1 : 1	1.5	DMSO–H_2O	60	13
9	1 : 1	1.5	DMSO–MeOH	60	70
10	1 : 1	1.5	DMSO	60	60
11	1 : 1	1.5	MeOH	60	63
12	1 : 1.5	1.5	DMSO–THF	60	51
13[d]	1.5 : 1	1.5	DMSO–THF	60	92

[a] General procedure: CAN (0.5–1.5 mmol, 0.5–1.5 equiv., 274–822 mg) was added to the solution of vinyl azide **1a** (1.0 mmol, 1.0 equiv., 145–218 mg) and sodium benzenesulfinate **2a** (1.0–1.5 mmol, 1.0–1.5 equiv., 164–246 mg) in 10 mL of DMSO–THF (1 : 1), DMSO–MeCN (1 : 1), DMSO–H_2O (1 : 1), DMSO–MeOH (1 : 1), DMSO, MeOH under magnetic stirring. The reaction mixture was stirred for 30–90 min at room temperature. [b] Yields were determined by ^1H NMR using 1,4-dinitrobenzene as an internal standard. [c] Reaction mixture was heated to 40 °C. [d] **1a** (1.5 mmol, 218 mg), **2a** (1.0 mmol, 164 mg), CAN (1.5 mmol, 822 mg) were used.

lysis, which showed that the resulting azine **3aa** was a diastereoisomer with a *Z*,*Z*′-configuration (see ESI† for details). Usage of 0.5 equiv. of CAN resulted in **3aa** yield decrease to 43% (entry 2), while application of 1.5 equivalent provided **3aa** in an 80% yield (entry 3). When the reaction mixture was stirred for 30 minutes, **3aa** yield dropped (entry 4). Raise in the reaction time to 90 minutes did not lead to significant change in the process efficiency (entry 5). Heating the reaction mixture to 40 °C was also ineffective to achieve better yield of **3aa** (entry 6). When different from DMSO-THF solvents were applied (entries 7–11), no increase in **3aa** product yield was observed. Finally, variation of the starting reagents molar ratio (entries 12 and 13) demonstrated that application of 1.5 excess of vinyl azide **1a** resulted in **3aa** formation in almost quantitative yield (92%, entry 12). Thus, usage of 1.5 equivalents of vinyl azide **1a**, 1.5 equivalents of CAN, DMSO-THF as the solvent, and 60 minutes of reaction time can be considered as optimal conditions for CAN-mediated synthesis of sulfonyl azine **3aa** from vinyl azide **1a** and sodium sulfinate **2a** (Table 1, entry 13).

With the optimized reaction conditions in hand (Table 1, entry 13), we have studied a scope of the substrates compatible with the developed transformation (Table 2). As we can see, a wide variety of both vinyl azides **1** and sodium sulfinates **2** successfully enter CAN-mediated sulfonylation. It is worth noting, that under developed conditions, azines **3** are formed predominantly as *Z*,*Z*′-diastereoisomers with a minor admixture of *E*,*Z*- and *E*,*E*′-isomers. In most cases, yields of the desired sulfonyl azines **3** exceeded 80%. Aromatic sulfinates **2** with electron-donating and electron-withdrawing groups gave the target products **3aa–3af** in 64–86% yields. Similarly, naphthyl- and thienyl-substituted sulfinates **2g** and **2h** provided sulfonylated compounds **3ag** and **3ah** in 76% and 73% yields, respectively. Aliphatic sodium sulfinates were also effective in the developed process resulting in ketazines **3ai–3al** in 57–87% yields.

A variety of vinyl azides **1** were also tested in CAN-mediated sulfonylation. Both electron-donating and electron-withdrawing substituents at *meta*- and *para*-positions had no significant effect on the reaction efficiency. Yields of the final compounds **3ba–3na** were 62–96%. Presence of the substituents such as Cl^- and F^- at the *ortho*-position slightly decreased yields of the products **3oa** and **3pa**. Naphthyl- and 1,2-dihydronaphthyl derivatives **3qa** and **3ra** were formed in 86% and 51% yields, respectively. When aliphatic vinyl azide **1s** was applied in optimal conditions, a trace amount of azine product **3sa** was observed. In contrast, when 1-(1-azidovinyl) cyclohex-1-ene **1t** was used, azine product **3ta** was isolated in a 75% yield. Nevertheless, azine **3sa** was obtained in a 31% yield when twofold excess of CAN and sulfinate **2a** were applied.

It was also shown that developed optimal conditions could be efficiently scaled up (Table 2). When 7.5 mmol of vinyl azide **1a** (1088 mg) were subjected to CAN-mediated sulfonylation with 5 mmol of sodium benzenesulfinate **2a** (820 mg), 904 mg of the desired azine **3aa** were obtained (70% yield). The α-sulfonylated ketazine **3aa** was transformed into the corresponding β-ketosulfone **10aa** under acidic conditions (see ESI† for details).

Table 2 Scope of synthesized α-sulfonylated ketazines **3**[a,b]

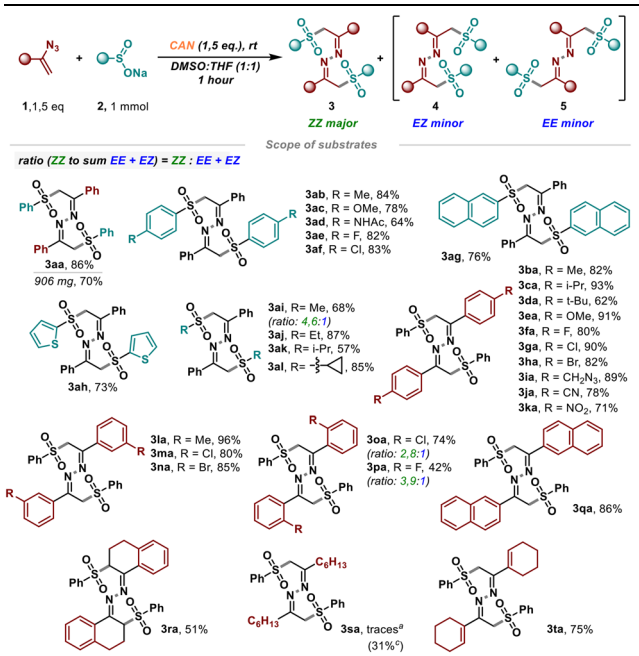

[a] General procedure: CAN (1.5 mmol, 822 mg) was added to the solution of vinyl azide **1** (1.5 mmol) and sodium sulfinate **2** (1 mmol) in 10 mL of DMSO–THF (1 : 1) under magnetic stirring. The reaction mixture was stirred for 60 min at 20–25 °C. [b] Isolated yields. [c] CAN (2 mmol, 1096 mg) was added to the solution of vinyl azide **1s** (1 mmol) and sodium sulfinate **2a** (2 mmol) in 10 mL of DMSO–THF (1 : 1) under magnetic stirring. The reaction mixture was stirred for 60 min at 20–25 °C.

2.2 Mechanistic elucidations

2.2.1 Radical trapping experiments. At the next stage, we conducted a series of control experiments to support the radical mechanism of the found process and detect key intermediates. Thus, the addition of radical traps TEMPO and BHT either completely suppressed the formation of dimerization product **3aa** or led to a partial decrease in its yield (Scheme 2A and B). In the case of BHT (Scheme 2B), the sulfonyl radical adduct was isolated and characterized.

Additionally, the formation of sulfonyl and iminyl radicals was confirmed with EPR spectroscopy, but signals were not

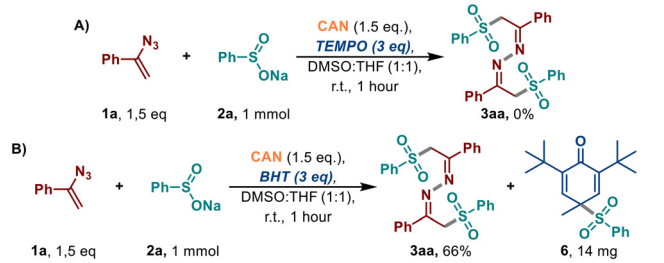

Scheme 2 Radical trapping experiments.

observed in the absence of a spin trapping reagent. Nevertheless, with the addition of the spin trapping reagent DMPO (5,5-dimethyl-1-pyrroline *N*-oxide) to the solution of **2a** and CAN, it was possible to detect the signal. On the basis of simulation, calculations, and literature analysis, the obtained spectrum was convincingly attributed to the sulfonyl radical spin adduct[57] **7** (g_{iso} = 2.0056, a_N = 0.99 mT, a_H = 1.97 mT) (Fig. 1A, see ESI† for details).

EPR spectrum was also recorded to detect the iminyl radical intermediate with the addition of a spin trapping reagent DMPO to the solution of **1a** and **2a**. When a stoichiometric amount of CAN solution was added, an EPR signal was identified. Additional EPR experiments, data analysis, simulation, and computations suggest that recorded spectrum can be attributed to the iminyl radical spin adduct[58] **8** (g_{iso} = 2.0058, a_N^1 = 0.27 mT, a_N^2 = 1.39 mT, a_H = 1.57 mT) (Fig. 1B, see ESI† for details).

Noteworthily, EPR spectra was also recorded for iminyl radical spin-adduct **8′** formed from aliphatic vinyl azide **1s**. Simulation and computations allowed us to support the presence of iminyl radical spin-adduct **8′** (g_{iso} = 2.0057, a_N^1 = 0.32 mT, a_N^2 = 1.42 mT, a_H = 1.47 mT) (Fig. 1C, see ESI† for details).

2.2.2 Kinetics and thermodynamics of the sulfonyl radical addition to vinyl azide double bond. With key intermediates detected, we performed calculations for the substitution of the ligand in the coordination sphere of cerium(IV) ammonium nitrate by the sulfinate anion (Scheme 3A). As we can see, substitution of nitrate anion with sulfinate occurs with minor gains in energy. However, at the next stage, the transfer of an electron from the sulfinate ligand to the metal leads to the free sulfonyl radical with sufficient energy gains.

As shown earlier, the application of aliphatic vinyl azide **1s** under optimized conditions led to ketazine **3sa** in only a trace amount (Table 2). While the application of aromatic vinyl azides or aliphatic ones containing conjugated double bond

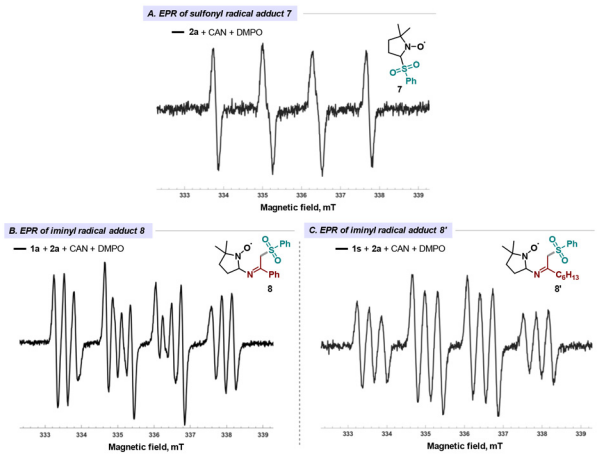

Fig. 1 The EPR spectra (X band, 9.4 GHz, room temperature, under Ar) of the reaction mixture of (A) **2a**, CAN, and DMPO; (B) **1a**, **2a**, CAN, and DMPO; (C) **1s**, **2a**, CAN, and DMPO in DMSO.

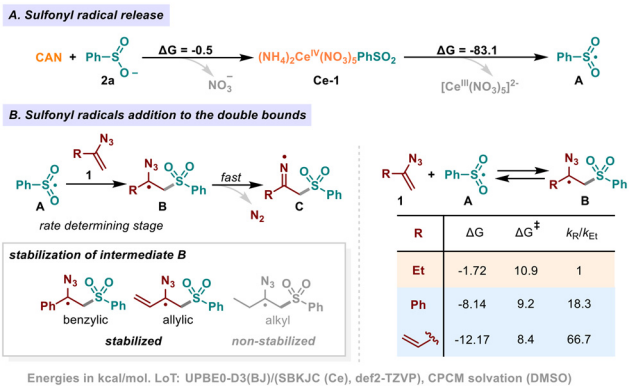

Scheme 3 (A) Computed free energies of sulfinate anion coordination and sulfonyl radical release. (B) Computed $\Delta G°$, $\Delta G^{‡}$ and relative rates (k_R/k_{Et}) of sulfonyl radical addition to the double bond of vinyl azides depending on substituents.

effectively resulted in the addition of sulfonyl radicals with the formation of ketazines **3aa–3ra** and **3ta**. For these reasons, we supposed that rapidly formed short-lived sulfonyl radicals **A** are intercepted more effectively by vinyl azides containing substituents at α-position that stabilize the C-centered radical **B** (Scheme 3B). The formation of intermediates **B** in sufficient concentration results in the accumulation of iminyl radicals **C** in the mixture with the subsequent radical N–N coupling (Scheme 3B). To confirm this assumption, we performed calculations of the activation and free energies of sulfonyl radical addition to the multiple bonds of vinyl azides depending on the substituents at α-position in intermediate **B** (Scheme 3B). As we can see, in the case of a saturated aliphatic substituent (ethyl), the addition of sulfonyl radical is thermodynamically and kinetically less preferable in comparison to phenyl and allyl substituted vinyl azides. Presence of phenyl or vinyl substituent at α-position to the carbon-centred radical **B** results in a slight decrease in the activation energy of addition to the double bond with larger free energy gains in contrast to the saturated aliphatic substituent. Taking all this into account, relative rate constants of sulfonyl radical addition to the double bonds of vinyl azides **1** have been calculated with Eyring–Polanyi equation. Thus, in the array of α-substituted radicals **B** relative rate constants (k_R/k_{Et}) rise in the order ethyl < phenyl < vinyl (Scheme 3B). These results support the postulate that the generation of iminyl radicals in required amount is governed by the reversibility and rate of sulfonyl radical addition to the vinyl azide double bond.

2.2.3 Thermodynamics of iminyl radical quenching by metal ions Ce(III) *vs.* Mn(II). Having two coordination sites iminyl radicals can act both as X- or L-type[59] ligands (Scheme 4A). For these reasons, the formal reduction of iminyl radical can occur when one coordinates as an X-type ligand according to the electronic demands of metal. To estimate the possibility of metal-to-ligand charge transfer (MLCT) for the previously disclosed Mn(III)-mediated[22,23,27,33] and present Ce(IV)-mediated processes we performed calculations for the

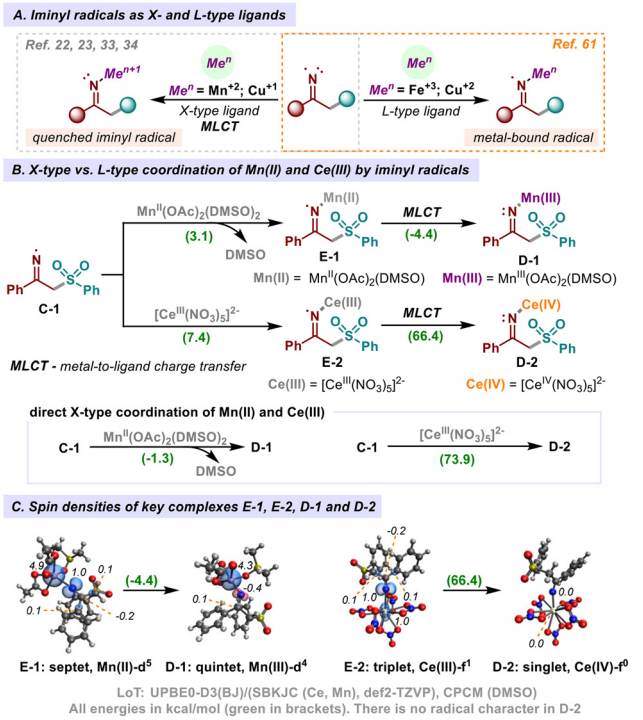

Scheme 4 (A) Iminyl radicals as an X- and L-type ligands (B) calculated free energies of metal-to-ligand charge transfer for Mn(II) and Ce(III) complexes. (C) Spin densities of key complexes D-1, D-2, E-1 and E-2.

complexes of Mn(II) and Ce(III) with iminyl radical **C-1** (Scheme 4B). There are two possible paths for the single electron transfer from metal to coordinated iminyl radical **C-1**. In the first case, the iminyl radical **C-1** coordinates with the metal as an L-type ligand, followed by metal-to-ligand charge transfer resulting in the formal reduction of **C-1**. Additionally, iminyl radical **C-1** could be directly coordinated by metal as an X-type ligand with loss of radical character.

As we can see, the coordination of **C-1** by Mn(II) as an L-type ligand (complex **E-1**) is slightly endergonic, while the subsequent stage of MLCT resulting in Mn(III)-complex **D-1** is slightly exergonic (Scheme 4B). In contrast, the coordination of **C-1** by Ce(III) as an L-type ligand (complex **E-2**) occurs without energy gains. Additionally, the subsequent MLCT stage that leads to the formation of Ce(IV)-complex **D-2** is highly endergonic. This likely indicates that Ce(III)-ions are neither effective at stabilizing the iminyl radical through L-type coordination nor at inducing the formal reduction of **C-1** *via* metal-to-ligand charge transfer.

The direct X-type coordination of the iminyl radical **C-1** by Mn(II) is slightly exergonic, which is potentially the main pathway for the formal reduction of the iminyl radical in the case of Mn(II) *via* the generation of **D-1** (Scheme 4B). In contrast, an analogous transformation involving charge transfer in the Ce(III)-complex **D-2** is highly endergonic.

Additional analysis of the spin density distribution in Mn(III)-complex **D-1** also revealed a significant loss of radical character on the nitrogen atom of the coordinated imine, in comparison to spin density distribution for complex **E-1** (Scheme 4C). For instance, the analogous loss of radical character process with Ce(IV)-complex **D-2** formation from Ce(III)-complex **E-2** is highly endergonic, which supports the unfeasibility of MLCT process in case of coordinated Ce(III).

Considering quantum calculations and the previously reported results, in which formal reduction of iminyl radicals by metal ions, such as Mn(II),[22,23,33] was proposed, we hypothesised that in our case iminyl radicals do not undergo the formal reduction step under the influence of formed Ce(III) ions. To support these speculations, we conducted a control experiment with the addition of possible iminyl radical quencher – $Mn(OAc)_2$ (Scheme 5A). When 1 mmol of manganese(II) acetate was added under optimal conditions, *N*-unsubstituted enaminosulfone **9aa** – the product of formal iminyl radical reduction – was detected in a 54% yield. The suppression of radical N–N coupling process in this case may suggest the pathway, under which iminyl radical coordinates with Mn(II) ions resulting in loss of its radical character. However, in the case of formed Ce(III), this pathway is presumably not implemented, thereby the process of iminyl radicals N–N coupling occurs. The reaction of **1a** with **2a** using $Mn(III)(OAc)_3$ led to **9aa** in 94% yield (Scheme 5B).

To summarize, the Mn(II) complex formed during the reduction of Mn(III) acts as an iminyl radical quencher, coordinating with subsequent metal-to-ligand charge transfer to form the Mn(III)-imine complex **D-1**. In contrast, Ce(III)-complex, formed from cerium(IV) ammonium nitrate, do not coordinate as L-type or X-type ligands with the radical **C-1**, thereby avoiding the loss of its radical character.

2.3 Proposed mechanism

Based on the control experiments, calculations and literature data, we proposed the mechanism for the developed transformation (Scheme 6). First, the sulfinate anion **2** is oxidized by cerium(IV) ammonium nitrate to form a sulfonyl radical **A** and Ce(III), which are quickly accumulated in the solution. The next reaction stage is rate determining and it includes sulfonyl radical **A** interception by the double bond of vinyl azide **1** to form a carbon-centred radical **B**. This radical undergoes rapid elimination of molecular nitrogen resulting in the key iminyl radical **C** generation.

The rate of iminyl radicals **C** accumulation depends on the efficiency of sulfonyl radicals **A** addition to the vinyl azide **1**

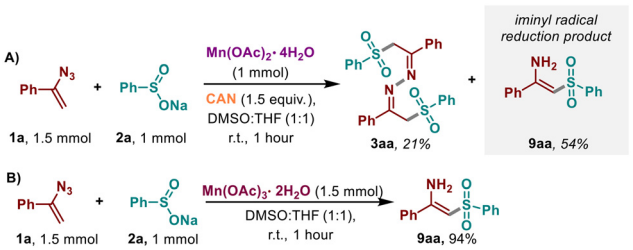

Scheme 5 N–N radical coupling suppression in the presence of manganese.

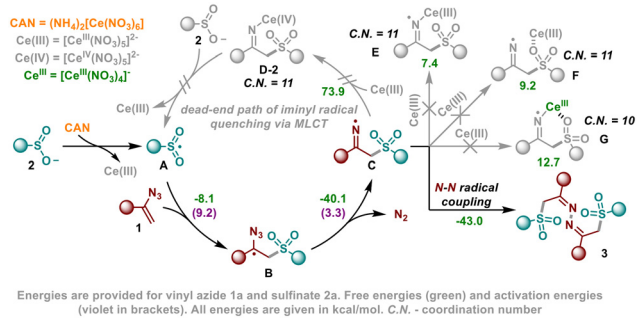

Scheme 6 Proposed mechanism.

double bond, which is directly linked to the substituent at the α-position relative to the formed radical center of intermediate **B**. To summarize, the more stable intermediate **B** is, the more iminyl radicals are formed. Iminyl radicals **C** accumulated in sufficient amount presumably cannot act as X-type ligands (otherwise, radical **C** would be reduced by Ce(III) with the formation of imine–cerium(IV) complex **D-2**). On the other hand, Ce(III)-ions presumably cannot stabilize iminyl radical **C** *via* L-type coordination on either nitrogen **E** or oxygen **F**. The formation of chelate complex **G** is also endergonic. For these reasons, coordination of iminyl radicals by formed Ce(III)-complex appeared to be unfeasible, affecting the performance of the radical N–N coupling process. Thereby, a free radical mechanism occurs and unquenched by Ce(III) iminyl radicals **C** dimerize to form azines **3**. Furthermore, the absence of iminyl radicals coordination by formed Ce(III)-complex and fast generation of iminyl radicals in high concertation may be responsible for the observed in the process radical N–N coupling. Due to this, ketazines **3** are formed selectively through stepwise radical C–S/N–N cascade coupling without the formation of N–S, C–N and S–S coupling products.

3 Conclusions

In conclusion, we have developed the synthesis of α-sulfonylated ketazines from vinyl azides and sodium sulfinates proceeding *via* stepwise radical C–S/N–N coupling cascade. Key intermediates of this process are sulfonyl and iminyl radicals. Sulfonyl radicals are generated through the oxidation of sodium sulfinates under the action of cerium(IV) ammonium nitrate. Iminyl radicals are in turn formed by addition of sulfonyl radicals to the double bonds of vinyl azides and further N_2 elimination. The conducted EPR study and radical trapping experiments confirmed the presence of sulfonyl and iminyl radicals in the reaction mixture. This transformation represents one of the rare facets of iminyl radical reactivity, namely, the dimerization of iminyl radicals while bypassing their formal reduction, intramolecular cyclization, and 1,*n*-HAT. Quantum chemical calculations highlighted the impact of the reversibility and rate of sulfonyl radical addition to the double bond of vinyl azides on the iminyl radical generation. Computed free energies of metal-to-ligand charge transfer (MLCT) and analysis of spin densities distribution of the coordinated metals allowed us to support the hypothesis that the selective N–N coupling of iminyl radicals is enabled by the inertness of Ce(III) towards coordination with iminyl radicals and the inaccessibility of charge transfer. On the other hand, Mn(II) coordinates with iminyl radicals, converting them into enamines that have been shown in previous studies. We believe that insights into the reactivity of iminyl radicals towards Ce(III) or Mn(II) ions, formed during the reduction of Ce(IV) or Mn(III), can provide a better understanding of the transformations involving iminyl radicals in the presence of widely used metal-based oxidants.

Data availability

The data supporting this article have been included as part of the ESI.† Crystallographic data for **3aa** has been deposited at the Cambridge Crystallographic Data Centre, under deposition number 2429110† and can be obtained from **https://www.ccdc.cam.ac.uk/structures**.

Conflicts of interest

There are no conflicts to declare.

Acknowledgements

This work was supported by the Russian Science Foundation (Grant No. 24-43-00111). Crystal structure determination was performed in the Department of Structural Studies of Zelinsky Institute of Organic Chemistry, Moscow. This work has been carried out using computing resources of the federal collective usage center Complex for Simulation and Data Processing for Mega-science Facilities at NRC "Kurchatov Institute".

References

1 W.-C. C. Lee and X. P. Zhang, Metalloradical Catalysis: General Approach for Controlling Reactivity and Selectivity of Homolytic Radical Reactions, *Angew. Chem., Int. Ed.*, 2024, **63**, e202320243.
2 V. A. Vil', Y. A. Barsegyan, L. Kuhn, A. O. Terent'ev and I. V. Alabugin, Creating, Preserving, and Directing Carboxylate Radicals in Ni-Catalyzed C(sp^3)–H Acyloxylation of Ethers, Ketones, and Alkanes with Diacyl Peroxides, *Organometallics*, 2023, **42**, 2598–2612.
3 L. Kuhn, V. A. Vil', Y. A. Barsegyan, A. O. Terent'ev and I. V. Alabugin, Carboxylate as a Non-innocent L-Ligand: Computational and Experimental Search for Metal-Bound Carboxylate Radicals, *Org. Lett.*, 2022, **24**, 3817–3822.
4 X. Qi, L. Zhu, R. Bai and Y. Lan, Stabilization of Two Radicals with One Metal: A Stepwise Coupling Model for

Copper-Catalyzed Radical–Radical Cross-Coupling, *Sci. Rep.*, 2017, **7**, 43579.
5 S. Zheng, Á. Gutiérrez-Bonet and G. A. Molander, Merging Photoredox PCET with Ni-Catalyzed Cross-Coupling: Cascade Amidoarylation of Unactivated Olefins, *Chem*, 2019, **5**, 339–352.
6 D. T. Ahneman and A. G. Doyle, C–H functionalization of amines with aryl halides by nickel-photoredox catalysis, *Chem. Sci.*, 2016, **7**, 7002–7006.
7 H. Tsurugi and K. Mashima, Renaissance of Homogeneous Cerium Catalysts with Unique Ce(IV/III) Couple: Redox-Mediated Organic Transformations Involving Homolysis of Ce(IV)–Ligand Covalent Bonds, *J. Am. Chem. Soc.*, 2021, **143**, 7879–7890.
8 V. Nair and A. Deepthi, Cerium(IV) Ammonium Nitrate - A Versatile Single-Electron Oxidant, *Chem. Rev.*, 2007, **107**, 1862–1891.
9 V. Sridharan and J. C. Menéndez, Cerium(IV) Ammonium Nitrate as a Catalyst in Organic Synthesis, *Chem. Rev.*, 2010, **110**, 3805–3849.
10 J. Fu, G. Zanoni, E. A. Anderson and X. Bi, α-Substituted vinyl azides: an emerging functionalized alkene, *Chem. Soc. Rev.*, 2017, **46**, 7208–7228.
11 H. Hayashi, A. Kaga and S. Chiba, α-Substituted vinyl azides: an emerging functionalized alkene, *J. Org. Chem.*, 2017, **82**, 11981–11989.
12 F. Gholami, F. Yousefnejad, B. Larijani and M. Mahdavi, Vinyl azides in organic synthesis: an overview, *RSC Adv.*, 2023, **13**, 990–1018.
13 B. Hu and S. G. DiMagno, Reactivities of vinyl azides and their recent applications in nitrogen heterocycle synthesis, *Org. Biomol. Chem.*, 2015, **13**, 3844–3855.
14 F.-L. Zhang, Y.-F. Wang, G. H. Lonca, X. Zhu and S. Chiba, Amide Synthesis by Nucleophilic Attack of Vinyl Azides, *Angew. Chem., Int. Ed.*, 2014, **53**, 4390–4394.
15 Z. Zhang, R. K. Kumar, G. Li, D. Wu and X. Bi, Synthesis of 4-Ynamides and Cyclization by the Vilsmeier Reagent to Dihydrofuran-2(3H)-ones, *Org. Lett.*, 2015, **17**, 6190–6193.
16 X. Zhu and S. Chiba, Construction of 1-pyrroline skeletons by Lewis acid-mediated conjugate addition of vinyl azides, *Chem. Commun.*, 2016, **52**, 2473–2476.
17 R. Dey and P. Banerjee, Lewis Acid Catalyzed Diastereoselective Cycloaddition Reactions of Donor-Acceptor Cyclopropanes and Vinyl Azides: Synthesis of Functionalized Azidocyclopentane and Tetrahydropyridine Derivatives, *Org. Lett.*, 2017, **19**, 304–307.
18 W. Chen, M. Hu, J. Wu, H. Zou and Y. Yu, Domino Approach for the Synthesis of Pyrrolo[1,2-α]pyrazine from Vinyl Azides, *Org. Lett.*, 2010, **12**, 3863–3865.
19 K. R. Dworakowski, S. Pisarek, S. Hassan and D. Gryko, Vinyl Azides as Radical Acceptors in the Vitamin B_{12}-Catalyzed Synthesis of Unsymmetrical Ketones, *Org. Lett.*, 2021, **23**, 9068–9072.
20 J. R. Donald and S. L. Berrell, Radical cyanomethylation via vinyl azide cascade-fragmentation, *Chem. Sci.*, 2019, **10**, 5832–5836.
21 S. A. Paveliev, A. I. Churakov, L. S. Alimkhanova, O. O. Segida, G. I. Nikishin and A. O. Terent'ev, Electrochemical Synthesis of O-Phthalimide Oximes from α-Azido Styrenes via Radical Sequence: Generation, Addition and Recombination of Imide-N-Oxyl and Iminyl Radicals with C–O/N–O Bonds Formation, *Adv. Synth. Catal.*, 2020, **362**, 3864–3871.
22 Y.-F. Wang, K. K. Toh, S. Chiba and K. Narasaka, Mn(III)-Catalyzed Synthesis of Pyrroles from Vinyl Azides and 1,3-Dicarbonyl Compounds, *Org. Lett.*, 2008, **10**, 5019–5022.
23 Y.-F. Wang, K. K. Toh, E. P. J. Ng and S. Chiba, Mn(III)-Mediated Formal [3 + 3]-Annulation of Vinyl Azides and Cyclopropanols: A Divergent Synthesis of Azaheterocycles, *J. Am. Chem. Soc.*, 2011, **133**, 6411–6421.
24 Y.-F. Wang, G. H. Lonca and S. Chiba, $PhI(OAc)_2$-Mediated Radical Trifluoromethylation of Vinyl Azides with Me_3SiCF_3, *Angew. Chem., Int. Ed.*, 2014, **53**, 1067–1071.
25 W. Shu, A. Lorente, E. Gómez-Bengoa and C. Nevado, Expeditious diastereoselective synthesis of elaborated ketones via remote Csp(3)-H functionalization, *Nat. Commun.*, 2017, **8**, 13832.
26 S. A. Paveliev, O. O. Segida, O. M. Mulina, I. B. Krylov and A. O. Terent'ev, Decatungstate-Catalyzed Photochemical Synthesis of Enaminones from Vinyl Azides and Aldehydes, *Org. Lett.*, 2022, **24**, 8942–8947.
27 O. M. Mulina, M. M. Doronin and A. O. Terent'ev, $Mn(OAc)_3$-Mediated Sulfonylation of Vinyl Azides Resulting in *N*-Unsubstituted Enaminosulfones, *ChemistrySelect*, 2021, **6**, 10250–10252.
28 Z. Fang, Y. Zhang, Z. Zhang, Q. Song, Y. Wu, Z. Liu and Y. Ning, Synthesis of *gem*-Disulfonyl Enamines via an Iminyl-Radical-Mediated Formal 1,3-HAT/Radical Coupling Cascade, *Org. Lett.*, 2022, **24**, 6374–6379.
29 Y. Liao, Y. Ran, G. Liu, P. Liu and X. Liu, Transition-metal-free radical relay cyclization of vinyl azides with 1,4-dihydropyridines involving a 1,5-hydrogen-atom transfer: access to α-tetralone scaffolds, *Org. Chem. Front.*, 2020, **7**, 3638–3647.
30 Y.-Q. Tang, J.-C. Yang, L. Wang, M. Fan and L.-N. Guo, Ni-Catalyzed Redox-Neutral Ring-Opening/Radical Addition/Ring-Closing Cascade of Cycloketone Oxime Esters and Vinyl Azides, *Org. Lett.*, 2019, **21**, 5178–5182.
31 J. C. Yang, J. Y. Zhang, J. J. Zhang, X. H. Duan and L. N. Guo, Metal-Free, Visible-Light-Promoted Decarboxylative Radical Cyclization of Vinyl Azides with N-Acyloxyphthalimides, *J. Org. Chem.*, 2018, **83**, 1598–1605.
32 Y. Ning, X.-F. Zhao, Y.-B. Wu and X. Bi, Radical Enamination of Vinyl Azides: Direct Synthesis of N-Unprotected Enamines, *Org. Lett.*, 2017, **19**, 6240–6243.
33 Y.-F. Wang and S. Chiba, Mn(III)-Mediated Reactions of Cyclopropanols with Vinyl Azides: Synthesis of Pyridine and 2-Azabicyclo[3.3.1]non-2-en-1-ol Derivatives, *J. Am. Chem. Soc.*, 2009, **131**, 12570–12572.
34 W.-L. Lei, K.-W. Feng, T. Wang, L.-Z. Wu and Q. Liu, Eosin Y- and Copper-Catalyzed Dark Reaction To Construct Ene-γ-Lactams, *Org. Lett.*, 2018, **20**, 7220–7224.

35 H.-M. Huang, M. H. Garduño-Castro, C. Morrill and D. J. Procter, Catalytic cascade reactions by radical relay, *Chem. Soc. Rev.*, 2019, **48**, 4626–4638.
36 O. M. Mulina, A. I. Ilovaisky, V. D. Parshin and A. O. Terent'ev, Oxidative Sulfonylation of Multiple Carbon-Carbon bonds with Sulfonyl Hydrazides, Sulfinic Acids and their Salts, *Adv. Synth. Catal.*, 2020, **362**, 4579–4654.
37 Z. Wang, Z. Zhang, W. Zhao, P. Sivaguru, G. Zanoni, Y. Wang, E. A. Anderson and X. Bi, Synthetic exploration of sulfinyl radicals using sulfinyl sulfones, *Nat. Commun.*, 2021, **12**, 5244.
38 Z. Zhang, X. Wang, P. Sivaguru and Z. Wang, Exploring the synthetic application of sulfinyl radicals, *Org. Chem. Front.*, 2022, **9**, 6063–6076.
39 K. A. Scott and J. T. Njardarson, Analysis of US FDA-Approved Drugs Containing Sulfur Atoms, *Top. Curr. Chem.*, 2018, **376**, 5.
40 J. Corpas, S.-H. Kim-Lee, P. Mauleón, R. G. Arrayás and J. C. Carretero, Beyond classical sulfone chemistry: metal- and photocatalytic approaches for C–S bond functionalization of sulfones, *Chem. Soc. Rev.*, 2022, **51**, 6774–6823.
41 X.-Q. Chu, D. Ge, Y.-Y. Cui, Z.-L. Shen and C.-J. Li, Desulfonylation via Radical Process: Recent Developments in Organic Synthesis, *Chem. Rev.*, 2021, **121**, 12548–12680.
42 P. Devendar and G.-F. Yang, Sulfur-Containing Agrochemicals, *Top. Curr. Chem.*, 2017, **375**, 82.
43 N. A. Meanwell, Synopsis of Some Recent Tactical Application of Bioisosteres in Drug Design, *J. Med. Chem.*, 2011, **54**, 2529–2591.
44 G. A. Patani and E. J. LaVoie, Bioisosterism: A Rational Approach in Drug Design, *Chem. Rev.*, 1996, **96**, 3147–3176.
45 K. Bredael, S. Geurs, D. Clarisse, K. De Bosscher and M. D'hooghe, Carboxylic Acid Bioisosteres in Medicinal Chemistry: Synthesis and Properties, *J. Chem.*, 2022, **2022**, 2164558.
46 S. Qin, M. Yang, M. Xu, Z.-H. Peng, J. Cai, S. Wang, H. Gao, Z. Zhou, A. S. K. Hashmi, W. Yi and Z. Zeng, Electrochemical *meta*-C–H sulfonylation of pyridines with nucleophilic sulfinates, *Nat. Commun.*, 2024, **15**, 7428.
47 M. J. Tilby, D. F. Dewez, L. R. E. Pantaine, A. Hall, C. Martínez-Lamenca and M. C. Willis, Photocatalytic Late-Stage Functionalization of Sulfonamides via Sulfonyl Radical Intermediates, *ACS Catal.*, 2022, **12**, 6060–6067.
48 K. Sun, X.-L. Chen, Y.-L. Zhang, K. Li, X.-Q. Huang, Y.-Y. Peng, L.-B. Qu and B. Yu, Metal-free sulfonyl radical-initiated cascade cyclization to access sulfonated indolo [1,2-*a*]quinolines, *Chem. Commun.*, 2019, **55**, 12615–12618.
49 L. Zheng, Z.-Z. Zhou, Y.-T. He, L.-H. Li, J.-W. Ma, Y.-F. Qiu, P.-X. Zhou, X.-Y. Liu, P.-F. Xu and Y.-M. Liang, Iodine-Promoted Radical Cyclization in Water: A Selective Reaction of 1,6-Enynes with Sulfonyl Hydrazides, *J. Org. Chem.*, 2016, **81**, 66–76.
50 M.-H. Huang, Y.-L. Zhu, W.-J. Hao, A.-F. Wang, D.-C. Wang, F. Liu, P. Wei, S.-J. Tu and B. Jiang, Visible-Light Photocatalytic Bicyclization of 1,7-Enynes toward Functionalized Sulfone-Containing Benzo[*a*]fluoren-5-ones, *Adv. Synth. Catal.*, 2017, **359**, 2229–2234.
51 W. Chen, X. Liu, E. Chen, B. Chen, J. Shao and Y. Yu, KI-mediated radical multi-functionalization of vinyl azides: a one-pot and efficient approach to β-keto sulfones and α-halo-β-keto sulfones, *Org. Chem. Front.*, 2017, **4**, 1162–1166.
52 P. Sivaguru, S. Cao, K. R. Babu and X. Bi, Silver-Catalyzed Activation of Terminal Alkynes for Synthesizing Nitrogen-Containing Molecules, *Acc. Chem. Res.*, 2020, **53**, 662–675.
53 O. M. Mulina, N. V. Zhironkina, S. A. Paveliev, D. V. Demchuk and A. O. Terent'ev, Electrochemically Induced Synthesis of Sulfonylated N-Unsubstituted Enamines from Vinyl Azides and Sulfonyl Hydrazides, *Org. Lett.*, 2020, **22**, 1818–1824.
54 X. Mu, S. Xie, X. Ye, S. Tao, J. Li and D. Jiang, Ketazine-Linked Crystalline Porous Covalent Organic Frameworks, *J. Am. Chem. Soc.*, 2024, **146**, 25118–25124.
55 S. S. Chourasiya, D. Kathuria, A. A. Wani and P. V. Bharatam, Azines: synthesis, structure, electronic structure and their applications, *Org. Biomol. Chem.*, 2019, **17**, 8486–8521.
56 M. Sennappan, V. Srinivasa Murthy, P. B. Managutti, P. Subhapriya, K. Gurushantha, P. C. Ramamurthy, B. Hemavathi, K. S. Anantharaju and A. Thakur, Facile synthesis of azines by carboxylic acid esters as catalyst and facilitation of intersystem crossing (ISC) in azines by azine chromophore, *Sci. Rep.*, 2024, **14**, 24656.
57 M. Y. Balakirev and V. V. Khramtsov, ESR Study of Free Radical Decomposition of N,N-Bis(arylsulfonyl)hydroxylamines in Organic Solution, *J. Org. Chem.*, 1996, **61**, 7263–7269.
58 J. Ke, Y. Tang, H. Yi, Y. Li, Y. Cheng, C. Liu and A. Lei, Copper-Catalyzed Radical/Radical $C(sp^3)$-H/P-H Cross-Coupling: alpha-Phosphorylation of Aryl Ketone O-Acetyloximes, *Angew. Chem., Int. Ed.*, 2015, **54**, 6604–6607.
59 P. Hong, X. Song, Z. Huang, K. Tan, A. Wu and X. Lu, Insights into the Mechanism of Metal-Catalyzed Transformation of Oxime Esters: Metal-Bound Radical Pathway vs Free Radical Pathway, *J. Org. Chem.*, 2022, **87**, 6014–6024.

